Journal of Hazardous Materials 444 (2023) 130453

Contents lists available at ScienceDirect

Journal of Hazardous Materials

journal homepage: www.elsevier.com/locate/jhazmat

Research Paper

Highly selective recovery of Ni(II) in neutral and acidic media using a novel Ni(II)-ion imprinted polymer

A. Giove [a,b,*], Y. El Ouardi [a], A. Sala [b], F. Ibrahim [b], S. Hietala [c], E. Sievänen [d], C. Branger [b,**], K. Laatikainen [a,e]

[a] Lappeenranta-Lahti University of Technology LUT, School of Engineering Science, Department of Separation Science, Yliopistonkatu 34, FIN-53850 Lappeenranta, Finland
[b] Université de Toulon, MAPIEM, Toulon, France
[c] University of Helsinki, Department of Chemistry, PB 55, FIN-00014 Helsinki, Finland
[d] University of Jyväskylä, Department of Chemistry, P.O. Box 35, FIN-40014, Finland
[e] Finnish Defence Research Agency, Paroistentie 20, FIN-34100 Lakiala, Finland

HIGHLIGHTS

- A novel chelating monomer based on 2-(aminomethyl)pyridine was synthesised.
- The complex formation between the monomer and Ni(II) was studied in situ.
- A new Ni(II)-IIP was produced by inverse suspension polymerization.
- Ni(II)-IIP demonstrated high adsorption capacity and selectivity towards Ni(II).
- Ni(II)-IIP showed good reusability up to five adsorption-desorption cycles.

GRAPHICAL ABSTRACT

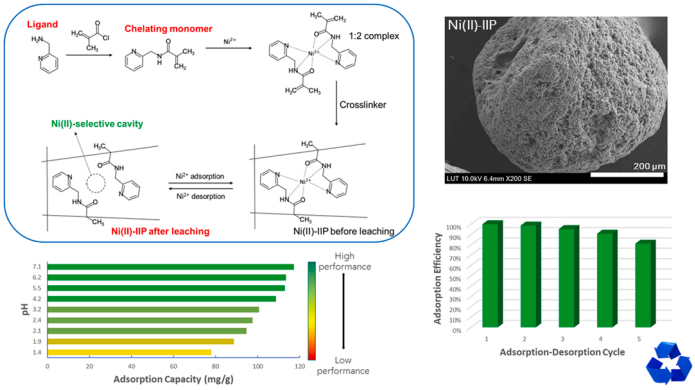

ARTICLE INFO

Editor: Arturo J Hernandez-Maldonado

Keywords:
Nickel
2-(aminomethyl)pyridine

ABSTRACT

In this work, an original ion-imprinted polymer (IIP) was synthetized for the highly selective removal of Ni(II) ions in neutral and acidic media. First a novel functional monomer (AMP-MMA) was synthetized through the amidation of 2-(aminomethyl)pyridine (AMP) with methacryloylchloride. Following Ni(II)/AMP-MMA complex formation study, the Ni(II)-IIP was produced via inverse suspension polymerization (DMSO in mineral oil) and

Abbreviations: AMP, 2-(aminomethyl)pyridine; AMP-MMA, 2-(aminomethyl)pyridine monomer; AIBN, 2,2-azobis(2-methylpropionitrile); DMSO, Dimethyl sulfoxide; EGDMA, Ethylene glycol dimethacrylate; FTIR, Fourier-Transform infrared spectroscopy; ICP-MS, Inductively coupled plasma mass spectroscopy; IIP, Ion Imprinted Polymer; MMA, Methyl methacrylate; HEPES, N-(2-hydroxyethyl)piperazine-N-2-ethanesulfonic acid; NIP, Non-Imprinted Polymer; PEGDMA, Polyethylene glycol dimethacrylate; SEM, Scanning electron microscopy; IARC, The International Agency for Research on Cancer; WHO, World Health Organization.

* Corresponding author at: Lappeenranta-Lahti University of Technology LUT, School of Engineering Science, Department of Separation Science, Yliopistonkatu 34, FIN-53850 Lappeenranta, Finland.
** Corresponding author.
E-mail addresses: alessio.giove@lut.fi (A. Giove), branger@univ-tln.fr (C. Branger).

https://doi.org/10.1016/j.jhazmat.2022.130453
Received 12 October 2022; Received in revised form 10 November 2022; Accepted 19 November 2022
Available online 21 November 2022

Solid-phase extraction
Porous polymer

characterized with solid state ^{13}C CPMAS NMR, FT-IR, SEM and nitrogen adsorption/desorption experiments. The Ni(II)-IIP was then used in solid-phase extraction of Ni(II) exploring a wide range of pH (from neutral to strongly acidic solution), several initial concentrations of Ni(II) (from 0.02 to 1 g/L), and the presence of competitive ions (Co(II), Cu(II), Cd(II), Mn(II), and Mg(II)). The maximum Ni(II) adsorption capacity at pH 2 and pH 7 reached values of 138.9 mg/g and 169.5 mg/g, that are among the best reported in literature. The selectivity coefficients toward Cd(II), Mn(II), Co(II), Mg(II) and Cu(II) are also very high, with values up to 38.6, 32.9, 25.2, 23.1 and 15.0, respectively. The Ni(II)-IIP showed good reusability of up to 5 cycles both with acidic and basic Ni(II) eluents.

1. Introduction

Nickel is a transition metal which can exist in 5 different oxidation states (−1, 0, +2, +3, +4), of which the most widely diffused in nature is the oxidation state + 2 (Muñoz and Costa, 2012). The widespread use of nickel in various sectors of the metallurgical industry (for example, in alloy and nickel-cadmium battery production, electroplating and welding) is resulting in high anthropological emissions into the environment, mainly as water soluble oxides and sulfides (Genchi et al., 2020; Sinicropi et al., 2010). Although nickel is necessary in small quantities for vital biological processes (such as plant growth and seed germination), overexposure is highly toxic to the environment and harmful for human health. High levels of nickel induce oxidative stress in plants and inhibit enzymatic, photosynthetic and chlorophyll activities (Sreekanth et al., 2013). Exposure to nickel compounds is associated with the development of nasal and lung cancers (Kasprzak et al., 2003). Nickel has been classified as a confirmed carcinogen by "The International Agency for Research on Cancer" (IARC) since 1990. In addition to its carcinogenic effects, nickel can induce allergic contact dermatitis and diseases of the respiratory and reproductive systems (Buxton et al., 2019).

The toxic effects of nickel are mainly associated with its presence in water solution in the oxidation state + 2 (Goodman et al., 2011). For this reason, the World Health Organization (WHO) has set increasingly stringent guidelines regarding the maximum permissible concentration of Ni(II) in water (70 μg/L) (World Health Organization, 2021). Metallurgical industries that discharge wastewater containing Ni(II) into the environment must follow strict environmental protection legislation, and there is therefore considerable interest in the development of new technologies for the recovery of Ni(II) from aqueous solutions.

Several alternatives for Ni(II) recovery from industrial wastewaters are available in literature, including chemical and electrochemical precipitation (Subbaiah et al., 2002; Blais et al., 2008), ion flotation (Doyle and Liu, 2003; Liu and Doyle, 2009), ion exchange (Revathi et al., 2012; Priya et al., 2009), membrane filtration (ultrafiltration, reverse osmosis, and nanofiltration) (Landaburu-Aguirre et al., 2012; Mohsen-Nia et al., 2007; Murthy and Chaudhari, 2008) and adsorption (Islam et al., 2019; Raval et al., 2016; Tuzen et al., 2009). These technologies all suffer from major disadvantages such as secondary pollution, large space requirements, high energy consumption, low capacity and, above all, poor selectivity in the presence of other competitive ions, which leads to lower Ni(II) extraction efficiency and an increase in recovery costs.

In the last two decades, many research groups have worked on the synthesis of ion-imprinted polymers (IIP) for use as highly selective adsorbents in the solid-phase extraction of heavy metals in solution (Rao et al., 2006; El Ouardi et al., 2021; Fu et al., 2015; Wu et al., 2022). The high selectivity of IIPs stems from the simultaneous presence of a chelating ligand within the polymer structure that can specifically interact with the target ion and of complementary shape-and-size selective cavities formed around the target ion during the polymerization process (Branger et al., 2013). Generally, the first step in the synthesis of an IIP is the formation of a complex between a monomer containing one or more chelating groups and the target ion, which acts as a template. The complex is then copolymerized with an excess of crosslinker to form a three-dimensional network around the complex. Finally, the template ions are removed and cavities that are chemically and physically complementary to the target ion are thus formed.

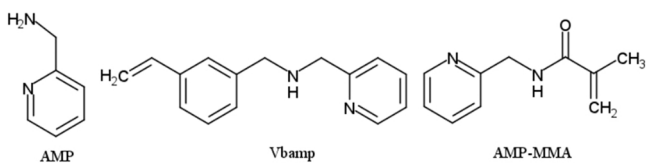

Fig. 1. AMP, Vbamp and AMP-MMA structures.

In this study, a new Ni(II)-IIP was synthesized for the recovery of Ni (II) ions in acidic and neutral conditions. The novel chelating monomer, hereinafter referred to as AMP-MMA, used for the synthesis of the Ni(II)-IIP was obtained through the reaction of the commercial ligand 2-(aminomethyl)pyridine (AMP) with methacryloylchloride (Fig. 1). The AMP ligand can act as an electron donor through its two nitrogen atoms and can form 1:1, 1:2 and 1:3 complexes with Ni(II) ions (Laatikainen et al., 2014). Moreover, its low basicity should allow polymer containing the ligand to have a low protonation degree even in strongly acidic conditions, and it can thus maintain good efficiency even at low pH (Sirola et al., 2008). In a previous work by this research group, AMP was functionalized with 3-vinylbenzaldehyde to produce a new functional monomer called Vbamp (Vinylbenzyl-amp) (Fig. 1) (Laatikainen et al., 2015). The Vbamp monomer was then used to produce IIPs at different Vbamp/Ni(II) stoichiometry to study the effect of different complexes on selectivity. Although the work provided valuable information for optimisation of pre-polymerization conditions in the synthesis of IIPs, the results obtained in terms of maximum adsorption capacity and performance at pH 4 (the most acidic conditions tested) were not sufficient to make it an industrially competitive adsorbent. The AMP-MMA monomer presented in this work is based on AMP ligand as well, but its structure deriving from functionalization with methacryloylchloride is markedly different from that of Vbamp. The Vbamp monomer is in fact a bidentate chelator characterized by the presence of 2 aromatic functions with high steric hindrance, while in AMP-MMA the vinyl function is provided by an acrylic group which also introduces the carbonyl group into the molecule and makes AMP-MMA a tridentate chelator (Fig. 1). From this structural difference, we therefore expect an increase in the performance of the new Ni(II)-IIP compared to the IIPs produced with Vbamp in the extraction of Ni(II) ions in both strongly acidic and neutral solutions.

2. Experimental

2.1. Reagents

The chemicals 2-(aminomethyl)pyridine (2-pycolylamine, 99%, AMP), dichloromethane (99.8%, anhydrous), triethylamine (99%), nickel nitrate hexahydrate (99.9%, $Ni(NO_3)_2{\cdot}6\,H_2O$), cadmium nitrate tetrahydrate (98%, $Cd(NO_3)_2{\cdot}4\,H_2O$), magnesium nitrate hexahydrate (99%, $Mg(NO_3)_2{\cdot}6\,H_2O$), 2,2-azobis(2-methylpropionitrile) (98%, AIBN), mineral oil (heavy) and $MgSO_4$ (99.5% anhydrous) were purchased from Sigma-Aldrich (Steinheim, Germany) and used without further purification. Cobalt nitrate hexahydrate (≥98%, $Co(NO_3)_2{\cdot}6\,H_2O$) and copper nitrate hemihydrate (98%, $Cu(NO_3)_2{\cdot}2.5\,H_2O$) were purchased from VWR (Fontenay-Sous-Bois,

France) and Alfa Aesar (Kandel, Germany), respectively, and used without further purification. N-(2-hydroxyethyl)piperazine-N-2-ethanesulfonic acid (≥99%, HEPES) and hydrochloric acid (37%, HCl) were purchased from Fisher Scientific (Loughborough, U.K.) and used without further purification. Manganese nitrate tetrahydrate (≥98.5%, $Mn(NO_3)_2{\cdot}6\ H_2O$) and dimethyl sulfoxide (99.9%, DMSO) were purchased from Merck (Darmstadt, Germany) and used without further purification. Methacryloylchloride (97%), ethylene glycol dimethacrylate (98%, EGDMA) and methyl methacrylate (99%, MMA), purchased from Alfa Aesar, Acros Organics (Geel, Belgium) and Sigma-Aldrich, respectively, were washed with a 10% solution of NaOH and dried with $MgSO_4$ to remove polymerisation inhibitors. All solutions were prepared with MilliQ water (Merck Millipore Q-POD). For all experiments, vessels (Corning® tubes, syringes, filters, etc.) were pre-cleaned with HNO_3 (10%, Analytical Grade) purchased from Fisher Scientific and then thoroughly rinsed with MilliQ water.

2.2. Apparatus

^1H and ^{13}C NMR spectra were obtained using a Bruker Advance 400-MHz spectrometer (Bruker France).

Solid state ^{13}C CPMAS NMR spectra were measured using a Bruker Avance III spectrometer operating at 500 MHz for protons using a double resonance CPMAS probehead. Samples were packed into 4 mm o. d. ZrO2 rotors plugged with KEL-F endcaps and spun at spinning frequency of 10 kHz. The length of the contact time for cross-polarization was 2 ms and variable amplitude cross-polarization ramped from 70% to maximum amplitude during contact time was used. During the acquisition period, the protons were decoupled using SPINAL-64 decoupling and the length of the acquisition was 27 ms. 24000 scans were collected with a 2 s relaxation delay and spectra externally referenced to adamantane.

FTIR spectra were recorded on a PerkinElmer FT-IR Frontier spectrometer equipped with the ATR sampling accessory. Each spectrum was collected in the range of 4000–400 cm^{-1} as result of an average of 8 scans with a resolution of 4 cm^{-1}.

UV-Vis absorption spectra for complex formation study were measured at 80 °C with an UV-Vis spectrophotometer (Agilent 8453, Jasco V670) equipped with a thermostated cuvette holder.

The surface morphologies of the Ni(II)-IIP and NIP were analyzed using a Hitachi SU3500 scanning electron microscope (SEM).

Particle diameter was measured with an Olympus SZX9 optical microscope by averaging the size of 20 particles for each polymer.

Specific surface area and pore size distribution were determined with BET and BJH methods using nitrogen adsorption/desorption isotherms at 77 K on a Micrometrics Gemini V analyzer.

Metal concentrations were determined using inductively coupled plasma mass spectroscopy (ICP-MS, Agilent 7900).

2.3. Synthesis of functional monomer

Methacryloylchloride (0.89 mL, 9.24 mmol) was dissolved in 30 mL of anhydrous dichloromethane and cooled in an ice bath with NaCl. Separately, AMP (1.00 g, 9.24 mmol) and trimethylamine (1.30 mL, 9.24 mol) were dissolved in 10 mL of anhydrous dichloromethane. This second solution was then poured dropwise into a flask containing the methacryloylchloride solution and stirred for 24 h under argon. The reaction product was washed three times with water and then dried with $MgSO_4$. The functional monomer AMP-MMA (0.80 g, 4.54 mmol, molar yield equal to 49%) was then obtained by removing the dichloromethane with a rotary evaporator and characterized by NMR analysis. ^1H NMR peaks (Fig. S1) ($CDCl_3$, 400 MHz) δ (ppm): 8.54 (d, H_1, 2-pyridine), 7.68 (t, H_3, 2-pyridine), 7.29 (d, H_4, 2-pyridine), 7.21 (t, H_2, 2-pyridine), 5.83 (m, H_6, 1-ethylene), 5.38 (m, H_7, 1-ethylene), 4.61 (d, H_5, 2-methylene), 2.03 (t, H_8, methyl).

2.4. Complex formation study

Study of complex formation between AMP-MMA and Ni(II) was carried out in DMSO. The Ni(II) was introduced into the solution using its nitrate salt $Ni(NO_3)_2{\cdot}6\ H_2O$ as a source. Samples were prepared in 3 mL glass cuvettes with a path length of 1 cm and UV-Vis spectra were collected at 80 °C in the range of 300–900 nm. The whole dataset consists of 13 UV-Vis spectra collected keeping the total concentration in the solution (AMP-MMA plus $Ni(NO_3)_2{\cdot}6\ H_2O$) equal to 0.1 M but varying the ratio between the two components (0.01–0.09 M of AMP-MMA with 0.09–0.01 of $Ni(NO_3)_2{\cdot}6\ H_2O$). Spectra of 0.1 M solution of the two components in DMSO at 80 °C were also collected. The UV-Vis spectra from each experiment were processed with HypSpec (Laatikainen et al., 2014, 2018; Gans et al., 1985) to extrapolate the distribution of the complexes at equilibrium and to estimate the stability constant values.

2.5. AMP-MMA polymerization test and incorporation rate

122 mg (0.695 mmol) of AMP-MMA were dissolved in 3 mL of DMSO-d_6. After 1 h of stirring under argon, 626 mg (6.255 mmol) of methyl methacrylate and 4 mg (0.024 mmol) of AIBN were added. In a three-neck round-bottom flask equipped with a head mixer, 30 mL of mineral oil was mixed at 750 rpm under argon atmosphere and pre-heated to 80 °C. The reaction mixture was then added quickly to start the polymerization. The polymerization was carried out for 24 h at 80 °C. Two intermediate samplings were done after 4 h and 6 h to follow the incorporation of AMP-MMA in the final product as a function of time. Intermediate reaction fractions and final reaction mixture remaining in the reactor after separation by decantation of mineral oil were analysed with ^1H NMR spectroscopy to determine the percentage of reacted AMP-MMA.

2.6. Synthesis of AMP-MMA NIP and Ni(II)-IIP

Synthesis of the Ni(II)-IIP and the corresponding NIP was carried out by inverse suspension polymerization (DMSO as a dispersed phase in a continuous phase of mineral oil) following the procedure described in a previous work (Laatikainen et al., 2015, 2018).

For the synthesis of the Ni(II)-IIP, the Ni(II)/AMP-MMA complex was prepared by dissolving 490 mg (2.78 mmol) of AMP-MMA and 404 mg (1.39 mmol) of $Ni(NO_3)_2{\cdot}6\ H_2O$ in 15 mL of DMSO. This solution was first stirred for 1 h under argon and then 4.5 mL of EGDMA (25.05 mmol) and 15 mg (0.09 mmol) of AIBN were added to form the solution to be dispersed during polymerization. In a three-neck round-bottom flask equipped with a head mixer, 120 mL of mineral oil was mixed at 750 rpm under argon atmosphere and pre-heated to 80 °C, after which the dispersed phase solution was added quickly to start the polymerization. Polymerization was carried out for 4 h at 80 °C. After polymerization, the formed IIP particles were vacuum filtered, washed with 50 mL of chloroform and extracted with a Soxhlet extractor for 24 h in a 1:1 chloroform-acetone mixture. To leach the Ni(II) ions, the polymer particles were washed, at 200 rpm agitation, 5 times with 40 mL 0.1 M HCl and then with ultrapure water for a total period of 24 h. Finally, the particles were dried in a vacuum oven at 25 °C for 24 h, which gave 3.2 g of dry polymer.

NIP particles were synthetised following the same procedure described for Ni(II)-IIP but omitting $Ni(NO_3)_2{\cdot}6\ H_2O$ from the polymerization medium, obtaining 3.3 g of dry polymer.

Poly-EGDMA (PEGDMA) was synthetised following the same procedure as for NIP but omitting the presence of AMP-MMA from the polymerization medium, obtaining 3.0 g of dry polymer.

2.7. Ni(II) solid-phase extraction

2.7.1. Ni(II) adsorption isotherm and effect of pH

The Ni(II) adsorption experiments were carried out at room

temperature over a wide nickel ion concentration range, from 0.02 to 1.00 g/L. 10 mg of either Ni(II)-IIP or NIP was introduced in 10 mL of a $Ni(NO_3)_2{\cdot}6\ H_2O$ solution. The mixtures were placed in 15 mL Corning© tubes and shaken with an orbital shaker at 120 rpm for 20 h. At the end of the adsorption experiments, the dispersions were centrifuged at 5000 rpm for 5 min. The supernatant was then filtered by syringe filtration using a 0.45 μm surfactant-free cellulose acetate filter. Metal concentrations were determined using ICP-MS. Samples for the ICP-MS analyses were diluted with a 1:1 (% v/v) mixture of concentrated HNO_3 and HCl. The effect of pH was assessed by performing adsorption experiments with two different Ni(II) ion concentrations (0.2 and 1 g/L) at different pH values. The pH was adjusted by introducing concentrated HCl or NaOH solutions.

The binding capacity at equilibrium q_e, which represents the amount of Ni(II) adsorbed per unit mass of the adsorbent, was calculated with Eq. 1:

$$q_e = \frac{(C_0 - C_e)}{m} \times V \quad (1)$$

where C_0 is the initial metal ion concentration in the solution, C_e is the metal ion concentration at equilibrium in the dissolved phase, m is the mass of adsorbent, and V is the volume of the solution.

The sorption data were analyzed using the models of Langmuir (Langmuir, 1918) and Freundlich (Freundlich, 1906). Langmuir's model (Eq. 2) is based on a homogeneous surface with a finite number of identical sites and assuming no interaction between adjacent sites. It is expressed as:

$$q_e = \frac{q_m K_L C_e}{1 + K_L C_e} \quad (2)$$

where q_m refers to the maximum adsorption capacity and K_L is the Langmuir constant.

The Freundlich model (Eq. 3) assumes that the adsorption occurs onto a heterogeneous surface and is expressed as:

$$q_e = K_F C_e^{1/n} \quad (3)$$

where K_F and n are Freundlich constants related to the adsorption capacity and adsorption strength, respectively.

2.7.2. Selectivity

To determine the selectivity toward Ni(II) of the Ni(II)-IIP and NIP, Ni(II) ion adsorption experiments were performed in the presence of other competitive ions in the solution, namely Co(II), Cu(II), Cd(II), Mn (II), and Mg(II). Each selectivity experiment was performed at pH 2 (adjusted with HCl solution) and pH 7 (controlled with HEPES buffer). The experiments were carried out at room temperature for 20 h, coupling Ni(II) ions with concentration of 0.01 g/L with one of the other competitive ions with concentrations of 0.01, 0.1, and 1 g/L, forming each time a binary solution.

The distribution coefficient (K_d) and selectivity coefficient (k) were calculated according to the Eqs. 4 and 5:

$$K_d = \frac{q_e}{C_e} \quad (4)$$

$$k = \frac{K_{d,\,Ni(II)}}{K_{d,\,M(II)}} \quad (5)$$

where $K_{d,\,Ni(II)}$ is the distribution coefficient of Ni(II), while $K_{d,\,M(II)}$ is the distribution coefficient of the competitive ion.

The effect of the ion imprinting method on selectivity was determined through the relative selectivity coefficient, k´(Eq. 6), corresponding to the ratio between the selectivity coefficients of the Ni(II)-IIP and NIP (Branger et al., 2013).

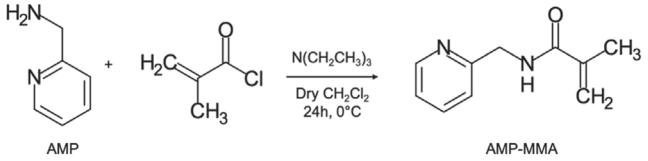

Scheme 1. Synthesis of AMP-MMA monomer.

$$k' = \frac{k_{IIP}}{k_{NIP}} \quad (6)$$

2.7.3. Ni(II)-IIP regeneration

Five regeneration cycles were carried out on Ni(II)-IIP adsorbent to investigate the reusability of the Ni(II)-IIP adsorbent. The effect of the leaching agent type and its concentration on the adsorption efficiency was evaluated for 5 regeneration cycles by performing the regeneration step with three different leaching agents, namely HNO_3 (1 and 3 mol/L), H_2SO_4 (1 and 3 mol/L), and NH_4OH (1 and 3 mol/L). In each regeneration cycle, the Ni(II)-IIP was leached with 10 mL of eluent for 30 min, rinsed three times with MilliQ water and finally dried at 60 °C for 24 h before the next adsorption/desorption cycle.

The adsorption efficiency in each cycle was calculated with Eq. 7:

$$Adsorption\ efficiency = \frac{q_{e,n}}{q_{e,1}} \quad (7)$$

where $q_{e,n}$ is the adsorption capacity of the n-cycle (with n = 1, 2, 3, 4 or 5) and $q_{e,1}$ is the adsorption capacity of the first cycle.

3. Results and discussion

3.1. Functional monomer synthesis and polymerization test

AMP was reacted with methacryloylchloride (Scheme 1) to introduce a methacrylic group into its structure, thus turning it from a ligand to a functional monomer. The success of the synthesis of AMP-MMA was assessed with ^{1}H NMR spectroscopy (Fig. S1), which confirmed the presence of the vinyl group protons (5.38 and 5.82 ppm) in the synthesized structure.

The reactivity of the AMP-MMA monomer was tested by copolymerizing it with MMA at the same conditions (AMP-MMA, comonomer and initiator concentrations, temperature, and DMSO/mineral oil ratio) as applied in the synthesis of Ni(II)-IIP and NIP. The aim of this test was to prove that the incorporation of AMP-MMA into the final products did not occur through physical trapping but through the creation of covalent bonds with the comonomer. The production of IIPs by trapping has been widely utilized in the last two decades as it permits direct use of commercially available ligands, thus avoiding the need for time-consuming synthesis of new functional monomers. The simplicity of the approach is however associated with a major disadvantage, namely the loss of the ligand during the ion template leaching step, reducing both the effectiveness of the IIP and its reliability over several adsorption cycles (Moussa et al., 2016).

The choice of MMA as a co-monomer for this test arose from the necessity to produce a linear polymer that could be easily solubilised and, consequently, analysed with liquid ^{1}H NMR spectroscopy (René et al., 2020). Moreover, the similarity of the chemical structure of MMA to that of EGDMA results in initial reactivity in the same order of magnitude (Ramelow and Pingili, 2010). Thus, the indications obtained copolymerizing AMP-MMA with MMA could be used with discrete confidence to design the copolymerization between AMP-MMA and EGDMA. Figs. S2 and S3 report the ^{1}H NMR spectra of the AMP-MMA and polymerization mixture after 4, 6 and 24 h in DMSO-d_6. The conversion (from monomer to polymer) of AMP-MMA and MMA and the molar fraction of AMP-MMA $X_{AMP-MMA}$ in the final product at different

Table 1
Time dependence of monomer conversion and $X_{AMP-MMA}$.

Reaction time	AMP-MMA conversion	MMA conversion	$X_{AMP-MMA}$
4 h	84.0%	93.2%	9.1%
6 h	90.0%	94.9%	9.5%
24 h	92.0%	95.7%	9.6%

Table 2
Stability constant values for AMP-MMA/Ni(II) complexes in DMSO at 80 °C.

Ni $(NO_3)_2$·6 H_2O/AMP-MMA	Stability constant value (log β)
1:1	8.49 ± 0.16
1:2	14.92 ± 0.33
1:3	/

polymerization time were calculated with Eqs. S1, S2 and S3, respectively, and is shown in Table 1. In copolymerization between AMP-MMA and MMA, reaction times longer than 4 h lead to minor variations in the $X_{AMP-MMA}$ values. Therefore, a reaction time of 4 h was also chosen for the copolymerization between AMP-MMA and EGDMA in production of the Ni(II)-IIP and NIP.

3.2. Complex formation study

The stoichiometry of the complex between the functional monomer and template ion greatly affects the selectivity of the IIP formed around it. Thus, it is preferable to optimize the pre-polymerization medium such that only the complex that leads to the highest adsorption efficiency is found in the solution. The stoichiometry in the pre-polymerization medium can be easily adjusted following in-situ study of complex formation, avoiding time-consuming complex isolation by conventional methods (Laatikainen et al., 2015, 2018).

To determine the optimum Ni/AMP-MMA ratio to be used in the Ni (II)-IIP pre-polymerization mixture, the formation of complexes between Ni$(NO_3)_2$·6 H_2O and AMP-MMA was studied in DMSO at 80 °C (the temperature at which the polymerization was then carried out).

Fig. S4 shows the complex distribution curves calculated with the HypSpec program at different Ni/AMP-MMA ratios including also the curves related to free Ni(II) ion and free AMP-MMA in solution. The estimated stability constant values of detected complexes are shown in Table 2.

In this study, it was only possible to detect complexes with Ni/AMP-MMA stoichiometry equal to 1:1 and 1:2 but 1:3 complexes were not detected. The 1:2 complex $[Ni(AMP\text{-}MMA)_2]^{2+}$ could be fully isolated using a Ni^{2+}/AMP-MMA ratio equal to 0.5. With this ratio, 99.6% of Ni^{2+} is included in the 1:2 complex, 0.3% forms the 1:1 complex, and no free nickel and just 0.1% free AMP-MMA are detected (Fig. S4). Since the 1:1 stoichiometry complex is geometrically non-specific in the monomer/metal ion interaction, and therefore precursor of IIPs with low selectivity, the 1:2 complex was selected for synthesis of the Ni(II)-IIP.

3.3. Synthesis and chemical characterization of Ni(II)-IIP and NIP

The Ni(II)-IIP and NIP were synthetised by inverse suspension copolymerization of AMP-MMA and EGDMA with and without $NiNO_3$·6 H_2O, respectively. For that purpose, DMSO was used as a dispersed phase in mineral oil as a continuous phase. The aim was to prepare particles of suitable size for the extraction application. The synthesis route to produce the Ni(II)-IIP is shown in Scheme 2.

Both products, Ni(II)-IIP and NIP, were characterized with FTIR (Fig. 2) and solid state ^{13}C CPMAS NMR (Fig. 3) and compared to PEGDMA. This polymer was prepared in similar conditions as the Ni(II)-IIP and NIP to facilitate their characterization.

In all the FTIR spectra of Fig. 2, the most intense PEGDMA bands can be easily identified, including the C═O and C-O stretching bands and the -OCH_2 deformation vibration band at 1725 cm^{-1}, 1144 cm^{-1} and 1460 cm^{-1}, respectively (Meouche et al., 2017). The presence AMP-MMA in both the Ni(II)-IIP and NIP is confirmed by the detection of typical pyridine and amine bands, including the C═C and C═N pyridine stretching bands at 1575 cm^{-1} and 1593 cm^{-1}, and the C-N aromatic amine stretching bands at 1298 cm^{-1} and 1320 cm^{-1}. As confirmed by the FTIR spectra of the Ni(II)-IIP before and after Ni(II) ion acidic leaching with HCl 0.1 M, the presence of Ni(II) does not affect the

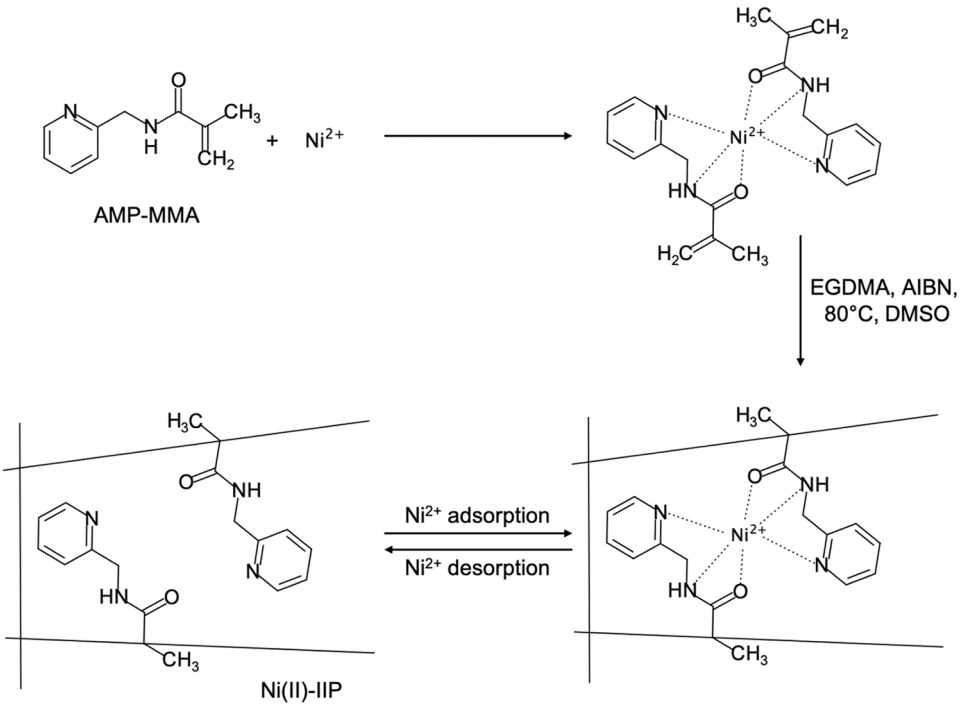

Scheme 2. Synthesis route of Ni(II)-IIP (the crosslinked polymer backbone of the imprinted polymer is schematized by the solid lines).

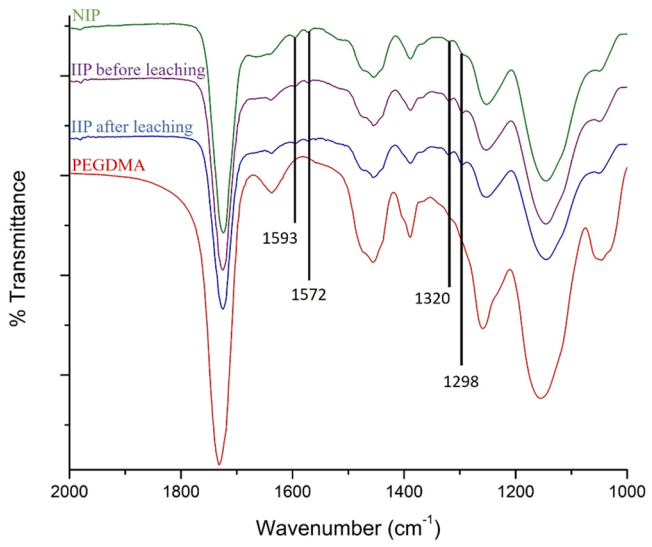

Fig. 2. FT-IR spectra of NIP, Ni(II)-IIP before and after leaching and PEGDMA.

vibrational modes of the final product, resulting in two identical FTIR spectra before and after the Ni(II) leaching. From this comparison, it also emerges that the 5 washes with HCl 0.1 M during a total period of 24 h did not modify the chemical composition of the Ni(II)-IIP, demonstrating good chemical resistance at strongly acidic pH.

In Fig. 3, all the spectra are characterized by the presence of typical PEGDMA bands, including the carbonyl carbon (C═O), the pending vinyl carbon (C═CH_2), the ester carbon (-COO-), the quaternary (>C<), methylene (-CH_2-) and methyl (-CH_3) carbons of the PEGDMA polymer chain at 177.1 ppm, 137.1 ppm, 62.9 ppm, 45.8 ppm, 24.5 ppm and 18.4 ppm, respectively (Chen et al., 2016). The presence of AMP-MMA in the Ni(II)-IIP and NIP was confirmed by the presence of peaks in the aromatic carbons zone that are not present in pure PEGDMA, including the pyridine carbon peaks at 157.9 ppm, 149.3 ppm and 124.5 ppm.

3.4. Morphological characterization of Ni(II)-IIP and NIP

The Ni(II)-IIP and NIP produced via inverse suspension polymerization resulted in near-spherical particles with average particle diameter of 1340 ± 598.72 μm and 915.25 ± 215.77 μm, respectively (Fig. S5 shows the particle size distributions determined with an optical microscope for the Ni(II)-IIP and NIP). The external morphology of the Ni(II)-IIP and NIP was studied by SEM (Fig. 4). The Ni(II)-IIP is characterized by an external surface that has high and regular porosity along the entire particles. The NIP, on the other hand, presents macroscopically continuous zones separated by superficial cracks.

The porosity of the two polymers was analysed with nitrogen adsorption/desorption experiments (Fig. 5). Isotherms for both polymers were of type IV with a hysteresis loop H4 in the IUPAC classification (Sing, 1985). This is indicative for mesoporous materials (pore diameter between 2 and 50 nm). This result was confirmed by the average pore diameter for the Ni(II)-IIP and NIP determined with the BJH method, which was equal to 9.0 nm and 7.0 nm, respectively. The BET surface area was similar for both polymers with values of 261 m^2/g for the Ni(II)-IIP and 268 m^2/g for the NIP, while the presence of Ni(II) as a template in the synthesis of the Ni(II)-IIP resulted in a higher total volume of pores equal to 0.59 cm^3/g compared with 0.47 cm^3/g for the NIP.

3.5. Ni(II) solid phase extraction

3.5.1. Effect of pH on Ni(II) adsorption

The effect of pH on Ni(II) adsorption was determined by studying the adsorption of Ni(II) by the Ni(II)-IIP and the NIP for Ni(II) solutions of 0.2 and 1.0 g/L with pH values ranging from 1.4 to 7.6 (Fig. 6). When the solution becomes more acidic (pH < 4), the degree of protonation of the AMP function in the polymers increases, diminishing the strength of the complex it can form with the Ni(II) ions in the solution due to growing electrostatic repulsion. Furthermore, the proton released in the solution by the acid can compete with Ni(II), reducing its complexation by AMP function. Indeed, a sharp drop or even a complete drop in Ni(II) adsorbents performance in strongly acidic solutions is typically reported in literature (Zhou et al., 2018; He et al., 2018, 2017; Jiang et al., 2006; Kumar et al., 2019). Even though there is an expected decrease in the Ni (II) adsorption efficiency at low pH also for the IIP produced in this work, the performance drop from pH 6 to pH 2 is very small, equal to 15%, widening the pH range of potential applications.

For each investigated pH, the binding capacity of the Ni(II)-IIP was always higher than the corresponding value for the NIP. This highlights

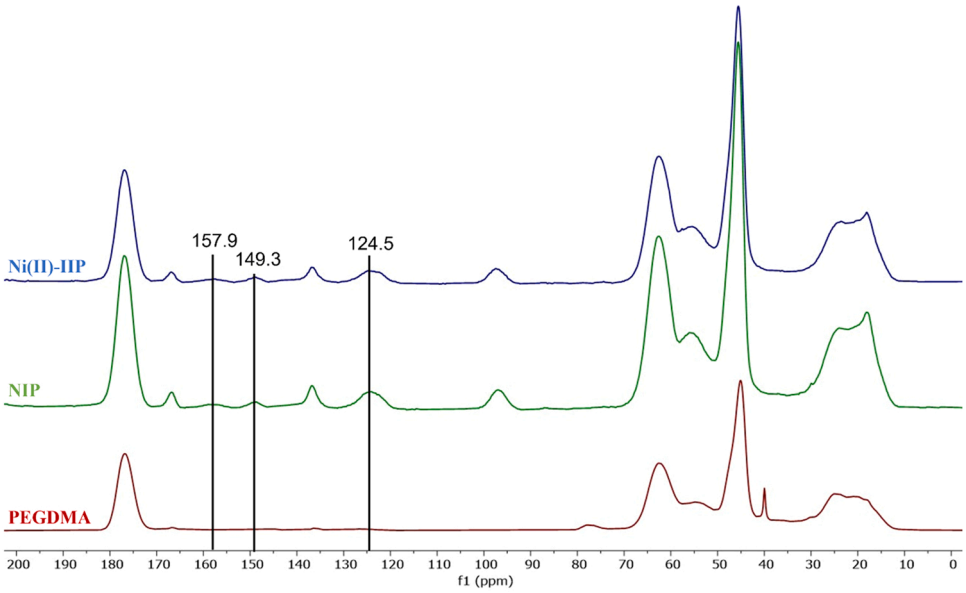

Fig. 3. ^{13}C CPMAS NMR spectra of Ni(II)-IIP, NIP and PEGDMA.

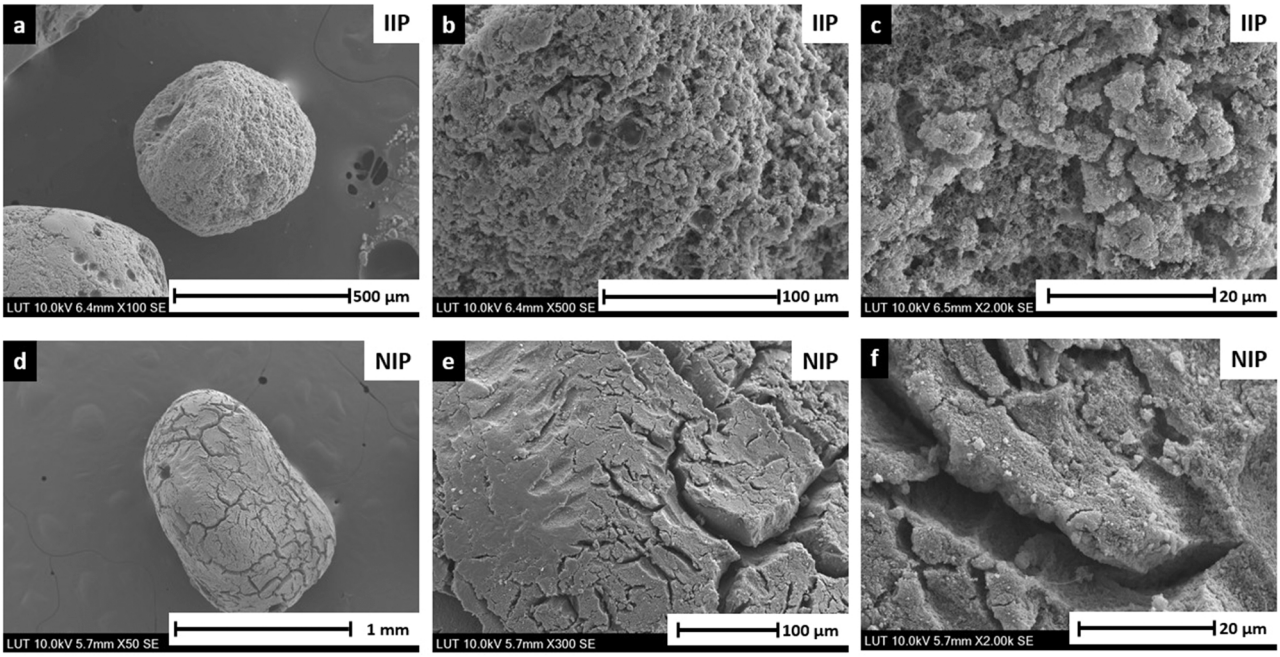

Fig. 4. SEM images of Ni(II)-IIP (a, b, and c) and NIP (d, e, f).

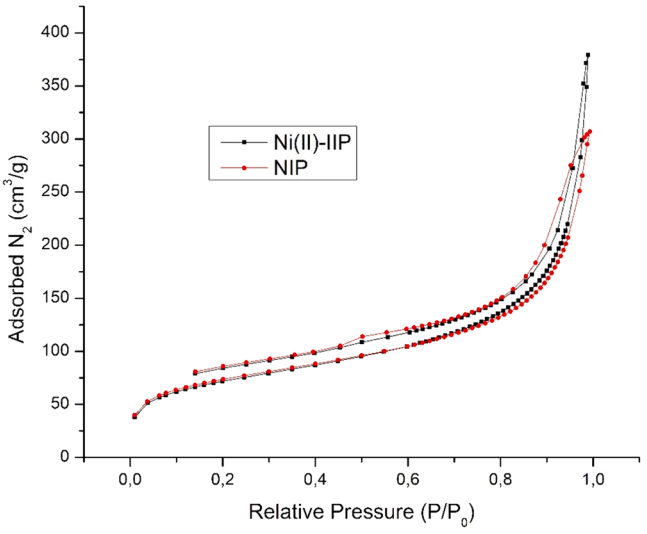

Fig. 5. Nitrogen adsorption/desorption isotherms of Ni(II)-IIP and NIP.

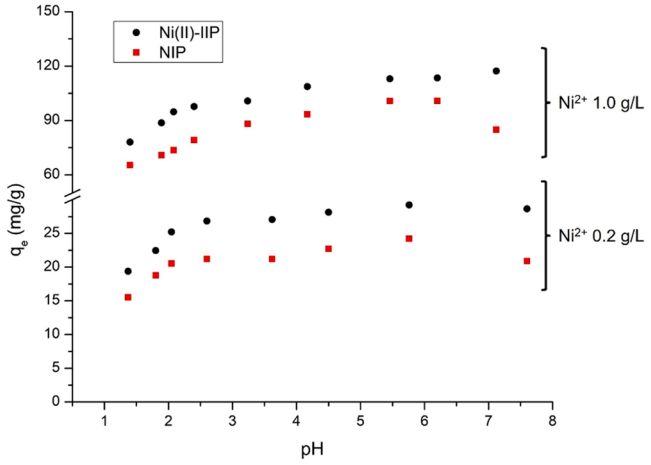

Fig. 6. Effect of pH on Ni(II) adsorption with Ni(II)-IIP (circles) and NIP (squares) at 2 different Ni(II) concentrations (1.0 g/L and 0.2 g/L).

an imprinting effect arising from the presence of the Ni(II) ion during polymerization of the Ni(II)-IIP. The imprinting factor, defined as the ratio between the binding capacity of the Ni(II)-IIP and NIP, showed minor variation along the whole pH range with an average value of 1.23 ± 0.07.

3.5.2. *Equilibrium isotherms at pH 2 and 7*

Before reaching saturation of all the adsorption sites, the binding capacity of porous materials depends on the concentration of the target ion in the solution and on the pH solution. For this reason, equilibrium isotherms related to Ni(II) adsorption were obtained by performing batch adsorption studies with the Ni(II)-IIP and NIP at pH 2 and pH 7 (Fig. 7). From the fitting parameters reported in Table 3, it appears that the experimental points for each isotherm are better interpolated by the Langmuir model as the correlation coefficient R^2 is always higher than that obtained after data interpolation with the Freundlich model. This means that the Ni(II) adsorption follows a monolayer adsorption pattern, with a maximum adsorption capacity for Ni(II)-IIP equal to 169.5 mg/g and 138.9 mg/g at pH 7 and 2, respectively.

Table 4 reports the maximum Ni(II) adsorption capacities of the Ni (II)-IIP produced in this work and those of other Ni(II) adsorbents described in literature. The reported values are those obtained in neutral conditions (pH 6–8) as the maximum adsorption capacity in strongly acidic solutions (pH 2 or similar) is not reported in these works. Comparison of the values in Table 4 shows that the Ni(II)-IIP proposed in this paper clearly has excellent Ni(II) adsorption capacity, with a q_e value higher than those reported in literature.

3.5.3. *Selectivity experiments*

The selectivity of the Ni(II)-IIP toward Ni(II) was studied at pH 2 and pH 7 in presence of Co(II), Cu(II), Cd(II), Mn(II), and Mg(II) as competitive ions in binary component solutions and with M(II)/Ni(II) concentration ratios of 1, 10 and 100 (Table 5). The highest selectivity performances with the Ni(II)-IIP were obtained at pH 7 with a M(II)/Ni (II) ratio equal to 100, reaching values of selectivity coefficients, k, of

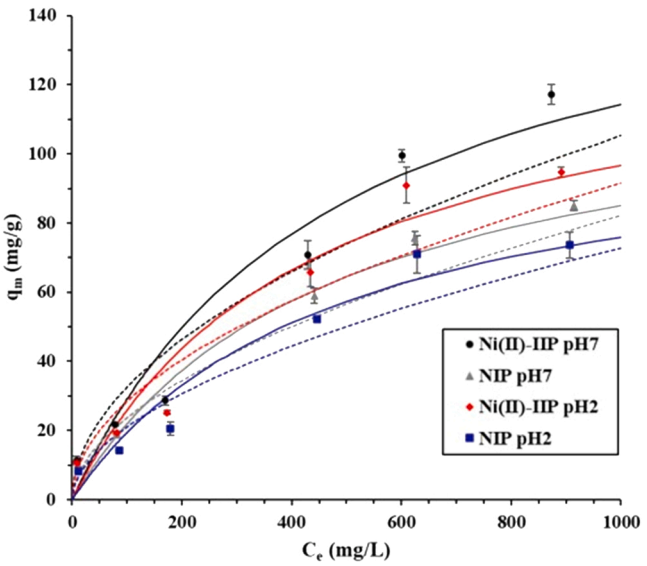

Fig. 7. Equilibrium isotherms for Ni(II) adsorption with the IIP and NIP at pH 2 and pH 7. Langmuir fitting is represented with continuous lines and Freundlich fitting with dashed lines. Experimental data are represented by the four different geometrical shapes.

38.6, 32.9, 25.2, 23.1 and 15.0 for Cd(II), Mn(II), Co(II), Mg(II) and Cu (II), respectively. The Ni(II)-IIP k values at pH 2 and M(II)/Ni(II) ratio equal to 100, had a similar trend to those at pH 7 and were only slightly reduced, confirming the high efficiency of the Ni(II)-IIP even in strongly acidic conditions.

From the results related to the adsorption of Ni(II) with the NIP with M(II)/Ni(II) ratio equal to 1 at both pH 2 and 7 (Table 5), it can be observed that k values are always higher than 1. This implies that, by its nature and even without the presence of the Ni(II)-complementary cavities generated with the imprinting technique, the AMP-MMA monomer prefers to interact with Ni(II) over the other competitive ions studied. Therefore, the monomer synthetised in this work is an optimal candidate to produce selective adsorbents for Ni(II). The increase of selectivity in the Ni(II)-IIP can be partially explained by the ionic radii dimensions of Ni(II) and the competitive ions. The Ni(II) ion radius and competitive ions radii follow the order: Cd(II)>Mn(II)>Co (II)>Cu(II)>Mg(II)>Ni(II), with values of 0.095, 0.083, 0.075, 0.073, 0.072, and 0.069 nm, respectively (Marcus, 1991). All the competitive ions have a bigger ionic radius than Ni(II), so they can hardly enter the shape-and-size selective cavities formed within the Ni(II)-IIP after Ni(II) leaching. Thus, the presence of Ni(II)-complementary cavities in the Ni (II)-IIP plays a fundamental role in selectivity. This results in average relative selectivity coefficients values in optimum conditions (ratio M (II)/Ni(II) equal to 100) of 2.0 ± 0.3 and 2.0 ± 0.4 at pH 2 and pH 7, respectively.

3.6. Ni(II)-IIP regeneration

Regeneration of the Ni(II)-IIP was evaluated over 5 adsorption/desorption cycles with HNO_3, H_2SO_4 and NH_4OH solutions at concentrations of 1 M and 3 M. It can be seen from the regeneration results (Fig. 8) that the best elution conditions were obtained with NH_4OH 3 M, with a decrease in adsorption efficiency of 1.3% in the second cycle and 18.8% in the fifth cycle. Good regeneration was also obtained using HNO_3 3 M, with an adsorption efficiency reduction of 3.1% in the second cycle and 19.2% in the fifth cycle. This result provides two different but similarly efficient options for Ni(II) leaching, which can be performed either in strongly acidic conditions, typically preferred when metal hydroxides precipitation needs to be avoided, or in strongly basic conditions.

4. Conclusions

A Ni(II)-IIP was produced via inverse suspension copolymerization of EGDMA with a novel functional monomer (AMP-MMA) based on 2-(aminomethyl)pyridine. The chemical composition of the Ni(II)-IIP was assessed with ^{13}C CPMAS NMR and FT-IR, which confirmed the incorporation of AMP-MMA in the poly-EGDMA network. The morphology of the polymer was investigated with SEM and nitrogen adsorption/desorption experiments, the results of which showed a different structure for the Ni(II)-IIP with respect to the non-imprinted polymer used as a reference. In particular, the Ni(II)-IIP had a higher total volume of pores as a result of the presence of Ni(II) ions during the polymerization procedure. The Ni(II)-IIP was then utilized for Ni(II) adsorption, which followed the Langmuir model with a maximum adsorption capacity equal to 169.5 mg/g and 138.9 mg/g at pH 7 and 2, respectively, among the highest values reported in literature. The selectivity of the Ni(II)-IIP was studied in the presence of Cd(II), Mn(II), Co(II), Mg(II) and Cu(II) as competitive ions, where selectivity coefficient values up to 38.6, 32.9, 25.2, 23.1 and 15.0, respectively, at pH 7 and slightly lower values at pH 2 were found. The binding and selectivity results demonstrated the high efficiency of the Ni(II)-IIP polymer synthetized in this work as a Ni(II) adsorbent in both neutral and acidic media. Finally, the reusability of the Ni(II)-IIP was tested over 5 Ni(II) adsorption/desorption cycles, which showed a regeneration efficiency of up to 98.7% after the first cycle and 81.2% in the fifth cycles, demonstrating the good chemical resistance of the polymer.

Table 4
Maximum adsorption capacities of different imprinted adsorbents for Ni(II) described in literature compared with the adsorbent produced in this work.

Chelating agent	$q_{e,max}$ (mg/g)	Reference
N-methacryloyl-histidine methyl ester	5.5	(Tamahkar et al., 2017)
3-aminopropyltrimethoxysilane	12.6	(Jiang et al., 2006)
chitosan and acrylic acid	19.9	(He et al., 2018)
2-acrylamido-2-methyl-1-propanesulfonic acid	20.3	(He et al., 2017)
acrylamide	81.7	(Liu et al., 2015)
diphenylcarbazide	86.3	(Zhou et al., 2018)
4- vinyl pyridine	125.0	(Kumar et al., 2019)
2-(aminomethyl)pyridine	169.5	Present study

Table 3
Langmuir and Freundlich parameters for Ni(II) sorption onto IIP and NIP at pH 2 and 7 at room temperature for 20 h.

Model	Parameter	Adsorbent			
Langmuir		IIP pH7	NIP pH7	IIP pH2	NIP pH2
	$q_{e,max}$ (mg/g)	169.49	125	138.88	112.36
	K_L	$2.07 * 10^{-3}$	$2.13 * 10^{-3}$	$2.29 * 10^{-3}$	$2.09 * 10^{-3}$
	R^2	0.948	0.954	0.945	0.954
Freundlich	1/n	0.510	0.5405	0.5076	0.539
	K_F	3.105	1.964	2.745	1.758
	R^2	0.902	0.932	0.901	0.919

Table 5
Distribution coefficients K_d, selectivity coefficients k and relative selectivity coefficients kfor Ni(II) adsorption with the Ni(II)-IIP and NIP at pH 2 and pH 7.

M (II)	**M(II)** / **Ni(II)**	Ni (II)-IIP pH 2			NIP pH 2			ḱpH 2	Ni (II)-IIP pH 7			NIP pH 7			ḱ pH 7
		$K_{d,Ni(II)}$	$K_{d,M(II)}$	k	$K_{d,Ni(II)}$	$K_{d,M(II)}$	k		$K_{d,Ni(II)}$	$K_{d,M(II)}$	k	$K_{d,Ni(II)}$	$K_{d,M(II)}$	k	
Co(II)	1	2.14	0.72	3.0	1.02	0.44	2.3	1.3	3.51	0.93	3.8	1.11	0.61	1.8	2.1
	10	1.72	0.42	4.1	0.76	0.19	4.1	1.0	3.05	0.54	5.7	0.83	0.18	4.7	1.2
	100	1.20	0.05	23.2	0.50	0.05	9.5	2.4	1.68	0.07	25.2	0.63	0.06	11.4	2.2
Mn(II)	1	2.20	0.44	5.0	0.92	0.43	2.2	2.3	3.07	0.52	5.9	1.35	0.44	3.1	1.9
	10	1.92	0.25	7.8	0.83	0.22	3.9	2.0	2.53	0.31	8.1	1.07	0.19	5.7	1.4
	100	1.34	0.05	27.3	0.65	0.04	15.3	1.8	1.95	0.06	32.9	0.83	0.05	17.2	1.9
Cd(II)	1	2.18	0.34	6.4	1.25	0.41	3.1	2.1	3.68	0.54	6.8	1.34	0.52	2.6	2.7
	10	1.85	0.21	8.9	1.07	0.24	4.4	2.0	2.90	0.31	9.3	1.13	0.22	5.2	1.8
	100	1.12	0.03	32.1	0.84	0.05	16.5	2.0	2.06	0.05	38.6	1.03	0.07	15.7	2.5
Cu(II)	1	1.88	1.49	1.3	0.81	0.66	1.2	1.0	2.94	1.58	1.9	0.96	0.69	1.4	1.3
	10	1.47	0.39	3.7	0.70	0.32	2.2	1.7	2.49	0.63	4.0	0.90	0.30	3.0	1.3
	100	0.96	0.06	14.8	0.47	0.05	8.8	1.7	1.42	0.09	15.0	0.74	0.07	10.5	1.4
Mg(II)	1	2.20	1.02	2.2	1.07	0.69	1.6	1.4	3.61	1.33	2.7	1.15	0.87	1.3	2.1
	10	3.46	0.66	5.2	1.87	0.47	4.0	1.3	5.97	1.12	5.4	2.11	1.12	1.9	2.8
	100	1.01	0.05	21.6	0.59	0.05	11.4	1.9	1.65	0.07	23.1	0.91	0.07	12.7	1.8

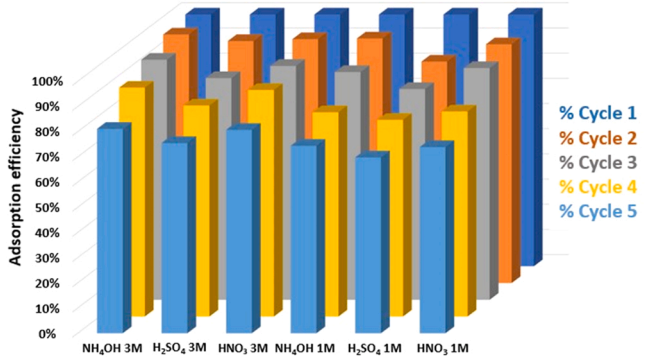

Fig. 8. Ni(II)-IIP adsorption/desorption cycles with NH_4OH, H_2SO_4 and HNO_3 1 M and 3 M as Ni(II) eluents.

Environmental implication

Overexposure to nickel is very dangerous for the environment as it induces oxidative stress in plants and inhibits enzymatic, photosynthetic and chlorophyll activities. No less important is the effect on human health since nickel is classified as confirmed carcinogen from "The International Agency for Research on Cancer". The toxic effects of nickel are mainly associated with its presence in the oxidation state + 2 and its recovery from acidic media results very complicated. The adsorbent proposed in this work demonstrated a high efficiency in Ni(II) recovery from acidic and neutral solutions and can therefore provide a valuable contribution to its remediation.

CRediT authorship contribution statement

Alessio Giove: Synthesis and characterization of monomer and polymers, Polymer application, Data curation, Writing – original draft, Writing – review & editing. **Youssef El Ouardi**: Polymer application, Writing – review & editing. **Alexandre Sala**: Monomer synthesis, Writing – review & editing. **Farah Ibrahim**: Polymer characterization, Writing – review & editing. **Sami Hietala**: Polymer characterization, Writing – review & editing. **Elina Sievänen**: Monomer characterization. **Catherine Branger**: Supervision, Project administration, Writing – review & editing. **Katri Laatikainen**: Supervision, Project administration, Writing – review & editing.

Declaration of Competing Interest

The authors declare that they have no known competing financial interests or personal relationships that could have appeared to influence the work reported in this paper.

Data Availability

Data will be made available on request.

Acknowledgements

The authors are thankful to the Academy of Finland and to Business of Finland for financial support through the projects "New generation separation materials and sensors for environmental applications – Interactions between ligands and ions/molecules (core project 23B350E9YT10)" and "BATCircle2.0 - Finland-based Circular Ecosystem of Battery Metals (core project 23B350E9YT10)", respectively. The authors thank Prof. Peter Jones for providing language help.

Appendix A. Supporting information

Supplementary data associated with this article can be found in the online version at doi:10.1016/j.jhazmat.2022.130453.

References

World Health Organization, ed., Nickel in drinking-water. Background document for development of WHO Guidelines for drinking-water quality, 2021. ⟨https://www.who.int/publications/i/item/WHO-HEP-ECH-WSH-2021.6⟩.
Blais, J.F., Djedidi, Z., Cheikh, B.R., Tyagi, R.D., Mercier, G., 2008. Metals precipitation from effluents: review. Pract. Period. Hazard. Toxic. Radioact. Waste Manag. 12, 135–149. https://doi.org/10.1061/(ASCE)1090-025X(2008)12:3(135).
Branger, C., Meouche, W., Margaillan, A., 2013. Recent advances on ion-imprinted polymers. React. Funct. Polym. 73, 859–875.
Buxton, S., Garman, E., Heim, K.E., Lyons-Darden, T., Schlekat, C.E., Taylor, M.D., Oller, A.R., 2019. Concise Review of Nickel Human Health Toxicology and Ecotoxicology. Inorganics 7. https://doi.org/10.3390/inorganics7070089.
Chen, J., Zhao, C., Huang, H., Wang, M., Ge, X., 2016. Highly crosslinked poly (ethyleneglycol dimethacrylate)-based microspheres via solvothermal precipitation polymerization in alcohol–water system. Polym. (Guildf.) 83, 214–222. https://doi.org/10.1016/j.polymer.2015.12.028.
Doyle, F.M., Liu, Z., 2003. The effect of triethylenetetraamine (Trien) on the ion flotation of Cu2+ and Ni2+. J. Colloid Interface Sci. 258, 396–403. https://doi.org/10.1016/S0021-9797(02)00092-9.
El Ouardi, Y., Giove, A., Laatikainen, M., Branger, C., Laatikainen, K., 2021. Benefit of ion imprinting technique in solid-phase extraction of heavy metals, special focus on the last decade. J. Environ. Chem. Eng. 9, 106548 https://doi.org/10.1016/j.jece.2021.106548.
Freundlich, H., 1906. Über die Adsorption in Lösungen. Z. Für Phys. Chem. 57, 385–470.
Fu, J., Chen, L., Li, J., Zhang, Z., 2015. Current status and challenges of ion imprinting. J. Mater. Chem. A 3, 13598–13627. https://doi.org/10.1039/C5TA02421H.
Gans, P., Sabatini, A., Vacca, A., 1985. SUPERQUAD: an improved general program for computation of formation constants from potentiometric data. J. Chem. Soc. {,} Dalt. Trans. 1195–1200. https://doi.org/10.1039/DT9850001195.

Genchi, G., Carocci, A., Lauria, G., Sinicropi, M.S., Catalano, A., 2020. Nickel: human health and environmental toxicology. Int. J. Environ. Res. Public Health 17. https://doi.org/10.3390/ijerph17030679.

Goodman, J.E., Prueitt, R.L., Thakali, S., Oller, A.R., 2011. The nickel ion bioavailability model of the carcinogenic potential of nickel-containing substances in the lung. Crit. Rev. Toxicol. 41, 142–174. https://doi.org/10.3109/10408444.2010.531460.

He, H., Gan, Q., Feng, C., 2017. Preparation and application of Ni(II) ion-imprinted silica gel polymer for selective separation of Ni(II) from aqueous solution. RSC Adv. 7, 15102–15111. https://doi.org/10.1039/c7ra00101k.

He, J., Shang, H., Zhang, X., Sun, X., 2018. Synthesis and application of ion imprinting polymer coated magnetic multi-walled carbon nanotubes for selective adsorption of nickel ion. Appl. Surf. Sci. 428, 110–117. https://doi.org/10.1016/j.apsusc.2017.09.123.

Islam, M.A., Awual, M.R., Angove, M.J., 2019. A review on nickel(II) adsorption in single and binary component systems and future path. J. Environ. Chem. Eng. 7, 103305 https://doi.org/10.1016/j.jece.2019.103305.

Jiang, N., Chang, X., Zheng, H., He, Q., Hu, Z., 2006. Selective solid-phase extraction of nickel(II) using a surface-imprinted silica gel sorbent. Anal. Chim. Acta 577, 225–231. https://doi.org/10.1016/j.aca.2006.06.049.

Kasprzak, K.S., Sunderman, F.W., Salnikow, K., 2003. Nickel carcinogenesis. Mutat. Res. Mol. Mech. Mutagen. 533, 67–97. https://doi.org/10.1016/j.mrfmmm.2003.08.021.

Kumar, A., Balouch, Abdullah, A., Pathan, A.A., 2019. Synthesis, adsorption and analytical applicability of Ni-imprinted polymer for selective adsorption of Ni2+ ions from the aqueous environment. Polym. Test. 77, 105871 https://doi.org/10.1016/j.polymertesting.2019.04.018.

Laatikainen, K., Udomsap, D., Siren, H., Brisset, H., Sainio, T., Branger, C., 2015. Effect of template ion–ligand complex stoichiometry on selectivity of ion-imprinted polymers. Talanta 134, 538–545. https://doi.org/10.1016/j.talanta.2014.11.050.

Laatikainen, K., Branger, C., Coulomb, B., Lenoble, V., Sainio, T., 2018. In situ complexation versus complex isolation in synthesis of ion imprinted polymers. React. Funct. Polym. 122, 1–8. https://doi.org/10.1016/j.reactfunctpolym.2017.10.022.

Laatikainen, M., Laatikainen, K., Reinikainen, S.-P., Hyvönen, H., Branger, C., Siren, H., Sainio, T., 2014. Complexation of nickel with 2-(Aminomethyl)pyridine at high zinc concentrations or in a nonaqueous solvent mixture. J. Chem. Eng. Data 59, 2207–2214. https://doi.org/10.1021/je500164h.

Landaburu-Aguirre, J., Pongrácz, E., Sarpola, A., Keiski, R.L., 2012. Simultaneous removal of heavy metals from phosphorous rich real wastewaters by micellar-enhanced ultrafiltration. Sep. Purif. Technol. 88, 130–137. https://doi.org/10.1016/j.seppur.2011.12.025.

Langmuir, I., 1918. The adsorption of gases on plane surfaces of glass, mica and platinum. J. Am. Chem. Soc. 345, 1361–1403.

Liu, Y., Meng, X., Liu, Z., Meng, M., Jiang, F., Luo, M., Ni, L., Qiu, J., Liu, F., Zhong, G., 2015. Preparation of a two-dimensional ion-imprinted polymer based on a graphene oxide/SiO2 composite for the selective adsorption of nickel ions. Langmuir 31, 8841–8851. https://doi.org/10.1021/acs.langmuir.5b01201.

Liu, Z., Doyle, F.M., 2009. Ion Flotation of Co2+, Ni2+, and Cu2+ Using Dodecyldiethylenetriamine (Ddien). Langmuir 25, 8927–8934. https://doi.org/10.1021/la900098g.

Marcus, Y., 1991. Thermodynamics of solvation of ions. Part 5.—Gibbs free energy of hydration at 298.15 K. J. Chem. Soc., Faraday Trans. 87, 2995–2999. https://doi.org/10.1039/FT9918702995.

Meouche, W., Laatikainen, K., Margaillan, A., Silvonen, T., Siren, H., Sainio, T., Beurroies, I., Denoyel, R., Branger, C., 2017. Effect of porogen solvent on the properties of nickel ion imprinted polymer materials prepared by inverse suspension polymerization. Eur. Polym. J. 87, 124–135. https://doi.org/10.1016/j.eurpolymj.2016.12.022.

Mohsen-Nia, M., Montazeri, P., Modarress, H., 2007. Removal of Cu2+ and Ni2+ from wastewater with a chelating agent and reverse osmosis processes. Desalination 217, 276–281. https://doi.org/10.1016/j.desal.2006.01.043.

Moussa, M., Pichon, V., Mariet, C., Vercouter, T., Delaunay, N., 2016. Potential of ion imprinted polymers synthesized by trapping approach for selective solid phase extraction of lanthanides. Talanta 161, 459–468. https://doi.org/10.1016/j.talanta.2016.08.069.

Muñoz, A., Costa, M., 2012. Elucidating the mechanisms of nickel compound uptake: a review of particulate and nano-nickel endocytosis and toxicity. Toxicol. Appl. Pharmacol. 260, 1–16. https://doi.org/10.1016/j.taap.2011.12.014.

Murthy, Z.V.P., Chaudhari, L.B., 2008. Application of nanofiltration for the rejection of nickel ions from aqueous solutions and estimation of membrane transport parameters. J. Hazard. Mater. 160, 70–77. https://doi.org/10.1016/j.jhazmat.2008.02.085.

Priya, P.G., Basha, C.A., Ramamurthi, V., Begum, S.N., 2009. Recovery and reuse of Ni (II) from rinsewater of electroplating industries. J. Hazard. Mater. 163, 899–909. https://doi.org/10.1016/j.jhazmat.2008.07.072.

Ramelow, U.S., Pingili, S., 2010. Synthesis of ethylene glycol dimethacrylate-methyl methacrylate copolymers, determination of their reactivity ratios, and a study of dopant and temperature effects on their conductivities. Polymers 2, 265–285. https://doi.org/10.3390/polym2030265.

Rao, T.P., Kala, R., Daniel, S., 2006. Metal ion-imprinted polymers—Novel materials for selective recognition of inorganics. Anal. Chim. Acta 578, 105–116. https://doi.org/10.1016/j.aca.2006.06.065.

Raval, N.P., Shah, P.U., Shah, N.K., 2016. Adsorptive removal of nickel(II) ions from aqueous environment: a review. J. Environ. Manag. 179, 1–20. https://doi.org/10.1016/j.jenvman.2016.04.045.

René, W., Lenoble, V., Chioukh, M., Branger, C., 2020. A turn-on fluorescent ion-imprinted polymer for selective and reliable optosensing of lead in real water samples. Sens. Actuators B Chem. 319, 128252 https://doi.org/10.1016/j.snb.2020.128252.

Revathi, M., Saravanan, M., Chiya, A.B., Velan, M., 2012. Removal of copper, nickel, and zinc ions from electroplating rinse water. CLEAN – Soil Air Water 40, 66–79. https://doi.org/10.1002/clen.201000477.

Sing, K.S.W., 1985. Reporting physisorption data for gas/solid systems with special reference to the determination of surface area and porosity (Recommendations 1984). Pure Appl. Chem. 57, 603–619. https://doi.org/10.1351/pac198557040603.

Sinicropi, M.S., Amantea, D., Caruso, A., Saturnino, C., 2010. Chemical and biological properties of toxic metals and use of chelating agents for the pharmacological treatment of metal poisoning. Arch. Toxicol. 84, 501–520. https://doi.org/10.1007/s00204-010-0544-6.

Sirola, K., Laatikainen, M., Lahtinen, M., Paatero, E., 2008. Removal of copper and nickel from concentrated ZnSO4 solutions with silica-supported chelating adsorbents. Sep. Purif. Technol. 64, 88–100. https://doi.org/10.1016/j.seppur.2008.08.001.

Sreekanth, T.V.M., Nagajyothi, P.C., Lee, K.D., V Prasad, T.N.V.K., 2013. Occurrence, physiological responses and toxicity of nickel in plants. Int. J. Environ. Sci. Technol. 10, 1129–1140. https://doi.org/10.1007/s13762-013-0245-9.

Subbaiah, T., Mallick, S.C., Mishra, K.G., Sanjay, K., Das, R.P., 2002. Electrochemical precipitation of nickel hydroxide. J. Power Sources 112, 562–569. https://doi.org/10.1016/S0378-7753(02)00470-6.

Tamahkar, E., Bakhshpour, M., Andaç, M., Denizli, A., 2017. Ion imprinted cryogels for selective removal of Ni(II) ions from aqueous solutions. Sep. Purif. Technol. 179, 36–44. https://doi.org/10.1016/j.seppur.2016.12.048.

Tuzen, M., Soylak, M., Citak, D., Ferreira, H.S., Korn, M.G.A., Bezerra, M.A., 2009. A preconcentration system for determination of copper and nickel in water and food samples employing flame atomic absorption spectrometry. J. Hazard. Mater. 162, 1041–1045. https://doi.org/10.1016/j.jhazmat.2008.05.154.

Wu, H., Lin, G., Liu, C., Chu, S., Mo, C., Liu, X., 2022. Progress and challenges in molecularly imprinted polymers for adsorption of heavy metal ions from wastewater. Trends Environ. Anal. Chem. 36, e00178 https://doi.org/10.1016/j.teac.2022.e00178.

Zhou, Z., Kong, D., Zhu, H., Wang, N., Wang, Z., Wang, Q., Liu, W., Li, Q., Zhang, W., Ren, Z., 2018. Preparation and adsorption characteristics of an ion-imprinted polymer for fast removal of Ni(II) ions from aqueous solution. J. Hazard. Mater. 341, 355–364. https://doi.org/10.1016/j.jhazmat.2017.06.010.